Small Molecule Therapeutics

Molecular Cancer Therapeutics

Fatostatin Displays High Antitumor Activity in Prostate Cancer by Blocking SREBP-Regulated Metabolic Pathways and Androgen Receptor Signaling

Xiangyan Li[1], Yi-Ting Chen[1], Peizhen Hu[1,2], and Wen-Chin Huang[1]

Abstract

Current research links aberrant lipogenesis and cholesterogenesis with prostate cancer development and progression. Sterol regulatory element-binding proteins (SREBP; SREBP-1 and SREBP-2) are key transcription factors controlling lipogenesis and cholesterogenesis via the regulation of genes related to fatty acid and cholesterol biosynthesis. Overexpression of SREBPs has been reported to be significantly associated with aggressive pathologic features in human prostate cancer. Our previous results showed that SREBP-1 promoted prostate cancer growth and castration resistance through induction of lipogenesis and androgen receptor (AR) activity. In the present study, we evaluated the anti–prostate tumor activity of a novel SREBP inhibitor, fatostatin. We found that fatostatin suppressed cell proliferation and anchorage-independent colony formation in both androgen-responsive LNCaP and androgen-insensitive C4-2B prostate cancer cells. Fatostatin also reduced *in vitro* invasion and migration in both the cell lines. Further, fatostatin caused G_2–M cell-cycle arrest and induced apoptosis by increasing caspase-3/7 activity and the cleavages of caspase-3 and PARP. The *in vivo* animal results demonstrated that fatostatin significantly inhibited subcutaneous C4-2B tumor growth and markedly decreased serum prostate-specific antigen (PSA) level compared with the control group. The *in vitro* and *in vivo* effects of fatostatin treatment were due to blockade of SREBP-regulated metabolic pathways and the AR signaling network. Our findings identify SREBP inhibition as a potential new therapeutic approach for the treatment of prostate cancer. *Mol Cancer Ther; 13(4); 855–66. ©2014 AACR.*

Introduction

Prostate cancer is the most prevalent malignancy diagnosed in males and the second leading cause of cancer-related mortality in the United States and Europe (1, 2). There is currently no effective therapy for advanced cancer progression. Epidemiologic evidence is mounting for a close relationship between dietary high fat intake and prostate carcinogenesis and lethal progression (3–5). Accumulated experimental research also suggests that activation of *de novo* lipogenesis (6–8) and cholesterogenesis (9–11) induces prostate cancer cell proliferation and promotes cancer development and progression. Therefore, pharmacologic intervention, blocking fatty acid and cholesterol anabolisms, could potentially be a novel therapy for malignant prostate cancer.

Authors' Affiliations: [1]Uro-Oncology Research Program, Department of Medicine, Samuel Oschin Comprehensive Cancer Institute, Cedars-Sinai Medical Center, Los Angeles, California and [2]Department of Pathology, Xijing Hospital, Fourth Military Medical University, Xi'an, Shaanxi, China

Note: Supplementary data for this article are available at Molecular Cancer Therapeutics Online (http://mct.aacrjournals.org/).

Corresponding Author: Wen-Chin Huang, Uro-Oncology Research Program, Department of Medicine, Samuel Oschin Comprehensive Cancer Institute, Cedars-Sinai Medical Center, Los Angeles, CA 90048. Phone: 310-423-7378; Fax: 310-423-8543; E-mail: wen-chin.huang@cshs.org

doi: 10.1158/1535-7163.MCT-13-0797

Sterol regulatory element-binding proteins (SREBP) are basic helix–loop–helix leucine (bHLH) zipper transcription factors that transcriptionally activate genes involved in fatty acid and cholesterol biosynthesis and homeostasis (12, 13). Precursor SREBPs are synthesized as endoplasmic reticulum (ER) membrane-bound forms. Through sequentially proteolytic cleavage by site-1 (S1P) and site-2 (S2P) proteases, the N-terminus of SREBPs translocate into the nucleus and trigger the expression of target genes having sterol regulatory elements (SRE), *cis*-acting elements in their 5′-flanking promoter regions (13, 14). Three isoforms of SREBPs have been identified, including SREBP-1a, SREBP-1c, and SREBP-2 (13, 15). SREBP-1a mainly regulates genes associated with fatty acid and cholesterol biosynthesis (12, 13). SREBP-2 is particularly involved in the transcriptional control of cholesterol anabolism (16). Overexpression of SREBP-1 has been found in human prostate cancer tissues and LNCaP xenograft tumor tissues during androgen refractory/castration-resistant progression (17, 18). In addition, our recent data showed that SREBP-1 and its nuclear form were highly elevated in clinical prostate cancer specimens with aggressive pathologic features compared with nontumor prostate tissues (18). Furthermore, SREBP-1 promoted cell viability and castration-resistant progression via alterations of lipogenesis, oxidative stress, and androgen receptor (AR) expression in prostate cancer cells (18). Previous reports revealed that SREBP-2

activity was increased in prostate cancer cells and targeting this activity altered cell membrane cholesterol content and inhibited signaling transduction mediated by cholesterol-rich lipid rafts (11, 17, 19–21). These discoveries provide a rationale for blocking SREBPs and their controlling metabolic and signaling pathways by pharmacologic intervention as a potential approach for prostate cancer therapy.

Fatostatin, a nonsterol diarylthiazole derivative, was originally developed from a chemical library to inhibit insulin-induced adipogenesis (22) and decreased the amounts of fatty acid, triglyceride and low-density lipoprotein and reduce body weight by perturbing the nuclear translocation of SREBP in obese mice with low cytotoxicity (23). Fatostatin has been shown to have the potential efficacy in glioma cells (24). Here, we report that fatostatin is a novel anti–prostate tumor agent that suppresses cell proliferation, tumorigenesis, and progression and induces apoptotic death in prostate cancer cells *in vitro* and *in vivo* by blocking SREBP activation and inhibiting fatty acid and cholesterol biosynthesis as well as AR signaling. This study indicates that inhibition of SREBP could be exploited as a promising therapy against malignant prostate cancer.

Materials and Methods

Cell lines and culture conditions

The human prostate cancer LNCaP cell line and C4-2B, a LNCaP lineage-derived bone metastatic subline, were kindly provided by Dr. Leland W.K. Chung (Cedars-Sinai Medical Center, Los Angeles, CA) in December 2010 (25). Mouse embryo fibroblast NIH-3T3 cells were purchased from the American Type Culture Collection (ATCC) in November 2013. These cell lines have not been further authenticated. LNCaP and C4-2B cells were cultured in T-Medium (Life Technologies). NIH-3T3 cells were cultured in Dulbecco's Modified Eagle Medium (DMEM; Life Technologies). All cell lines were grown in medium with 10% FBS (Atlanta Biologicals), 100 U/mL of penicillin and 100 μg/mL of streptomycin in a humidified atmosphere of 5% CO_2 at 37°C.

Compounds and reagents

Fatostatin (4-[4-(4-methylphenyl)-1,3-thiazol-2-yl]-2-propylpyridine hydrobromide) was purchased from Chembridge Corporation and its chemical structure is described in Supplementary Fig. S1. Ribonuclease A, propidium iodide (PI), Oil Red O and filipin III were purchased from Sigma-Aldrich. Annexin V-fluorescein isothiocyanate (FITC) Apoptosis Detection Kit I and Matrigel Basement Membrane Matrix were purchased from BD Biosciences. The Free Fatty Acid Quantification Kit and Cholesterol/Cholesterol Ester Detection Kit were obtained from Abcam. pHMGCoASyn-Luc construct was obtained from Dr. Hitoshi Shimano (University of Tsukuba, Tsukuba, Ibaraki, Japan). pFASN-700-Luc and pFASN-700-mutSRE-Luc constructs were obtained from Dr. Timothy F. Osborne of Sanford-Burnham Medical Research Institute (Orlando, FL). pLDLR-Luc and pLDLR-mutSRE constructs were obtained from Addgene.

Cell proliferation, clonogenicity, invasion, and migration assays

Prostate cancer cells were seeded on 96-well plates in triplicate and treated with vehicle or fatostatin for 72 hours. Cell proliferation was determined by MTS assay (Promega) according to the manufacturer's instructions. For the growth curve assay, cells were seeded on 24-well plates and treated with vehicle or fatostatin (2.5, 5, or 10 μmol/L) for 5 days. Cell numbers from triplicate wells were counted. For the clonogenic assay, cells were suspended in culture medium containing 0.3% agarose (FMC BioProducts) with vehicle or fatostatin, and placed on top of solidified 0.6% agarose in 6-well plates. The developed colonies were counted and recorded under a microscope after 3-week incubation. *In vitro* cell invasion or migration was determined in Boyden chambers precoated with growth factor–reduced BD Matrigel matrix (invasion assay) or collagen I (migration assay) as previously described (18). After incubation for 48 hours, invading or migrating cells were photographed and counted to calculate the relative cell invasion and migration.

Quantitative reverse transcription (qRT)-PCR analysis

Total RNA from each sample was isolated by RNeasy mini Kit (Qiagen). First-strand cDNA was synthesized from total RNA (1 μg) using SuperScript III reverse transcriptase (Life Technologies) with random hexamer primers. Quantitative PCR (qPCR) was performed on ABI 7500 Fast Real-Time PCR System using the SYBR Green PCR Master mix from Applied Biosystems. The oligonucleotide primer sets, including ATP citrate lyase (ACL), fatty acid synthase (FASN), stearoyl-CoA desaturase-1 (SCD-1), 3-hydroxy-3-methyl-glutaryl-CoA synthase 1 (HMGCS1), 3-hydroxy-3-methyl-glutaryl-CoA reductase (HMGCR), mevalonate kinase (MVK), mevalonate 5-pyrophosphate decarboxylase (MVD), low-density lipoprotein receptor (LDLR), insulin-induced gene 1 (INSIG1), SREBP cleavage activating protein (SCAP), and β-actin, are listed in Supplementary Table S1.

Western blot analysis

Cell lysates were prepared from prostate cancer cells as previously described (26) and Western blot analysis was performed using Mini-PROTEAN system (Bio-Rad). Primary antibodies against SREBP-1 (sc-8984), FASN (sc-48357), HMGCR (sc-33827), PSA (sc-7638) and β-actin (sc-47778; Santa Cruz Biotechnology), SREBP-2 (ab72856 and ab112046; Abcam), AR (PG-21; Millipore), and glyceraldehyde-3-phosphate dehydrogenase (GAPDH, 2118S; Cell Signaling Technology) and horseradish peroxidase–conjugated secondary antibodies (GE Healthcare Bio-Sciences Corp) were used and membranes were visualized using a chemiluminescence reagent (Amersham Biosciences).

Filipin and Oil Red O stainings

For filipin staining, cells were fixed, quenched with glycine, and stained by filipin solution (50 μg/mL in PBS) for 1 hour. The filipin staining images were visualized by fluorescence microscopy. For Oil Red O staining, cells treated with vehicle or fatostatin were stained by Oil Red O working solution and were examined by a phase-contrast microscope (18).

Quantification of fatty acid and total cholesterol

The amounts of fatty acid and cholesterol were measured using the Free Fatty Acid Quantification Kit and the Cholesterol/Cholesterol Ester Detection Kit according to the manufacturer's instructions (Abcam) in cells treated with vehicle or fatostatin (21).

Cell cycle and apoptosis analysis

Cells treated with vehicle or fatostatin for 48 hours were fixed, stained with PI (25 μg/mL), and analyzed by FACScan flow cytometer on the basis of 2N and 4N DNA content. Apoptotic cell death was assessed in cells treated with vehicle or fatostatin using Annexin V-FITC/PI Apoptosis Detection Kit (BD Bioscience). For caspase activity assay, cells treated with vehicle or fatostatin for 48 hours were measured for caspase-3/7 enzymatic activities using Caspase-Glo 3/7 Assay Systems (Promega). After treatment with vehicle or fatostatin for 72 hours, anti-caspase-9 (9502), anti-caspase-3 (9665), and PARP (9542) primary antibodies (Cell Signaling Technology) were used for Western blot analysis.

Luciferase activity assay

NIH-3T3 cells were transfected with pHMGCoASyn-Luc, pFASN-700-Luc, pFASN-700-mutSRE-Luc, pLDLR-Luc, and pLDLR-mutSRE constructs using Lipofectamine LTX Reagent (Life Technologies), following which they were treated with vehicle or fatostatin for 20 hours. The luciferase activity was measured by the Luciferase Assay Kit (Promega) and normalized to β-galactosidase luciferase activity by cotransfection of β-galactosidase control vector. pSRE-Luc, SREBP-1 (OriGene Technologies), SREBP-2, CMV500 A-SREBP1, and CMV500 A-SREBP2 (Addgene) vectors were transfected into cells as described above.

Mouse xenograft experiments

All animal experiments were performed in accordance with the protocol approved by the Cedars-Sinai Medical Center Institution Animal Care and Use Committee. Athymic nu/nu male mice (4-week-old; Taconic) were implanted subcutaneously with C4-2B cells (1×10^6). Tumor burdens were monitored by calipers and calculated using the formula $V = 1/2 \times \text{length} \times \text{width}^2$. Mice bearing C4-2B tumors with a mean volume of 100 mm^3 were randomly divided into vehicle control (sterile PBS) or fatostatin (15 mg/kg) groups with intraperitoneal injection for 42 days (23). Blood specimens were collected and serum PSA was determined by AIA-360 Immunoassay Analyzer (Tosoh Bioscience). At the end of the animal experiments, tumor xenografts were harvested for further analysis.

Immunohistochemical staining

Immunohistochemical (IHC) staining was performed as described previously (27). The paraffin-embedded C4-2B tumor tissue slides were analyzed for Ki67 (1:200 dilution; Abcam), cleaved PARP (1:30 dilution), HMGCR (1:50 dilution), FASN (1:100 dilution; Santa Cruz Biotechnology), AR (1:100 dilution; Millipore), and PSA (1:100 dilution; Vector Labs) expression. The percentages of Ki67-positive cells (proliferation) or cleaved PARP–positive cells (apoptosis) were calculated in five randomly selected microscopic fields at a ×200 magnification.

Statistical analysis

All quantitative results are expressed as means ± SD. Statistically significant differences were obtained using a two-tailed Student t test. A value of $P < 0.05$ was considered to be statistically significant in all experiments.

Results

Fatostatin inhibits cell proliferation, invasion, and migration of prostate cancer cells *in vitro*

To evaluate the effects of fatostatin on human prostate cancer cell lines with biologic heterogeneity, we carried out a set of cell survival assays by treating androgen-responsive LNCaP and androgen-independent C4-2B cells with fatostatin at serial dilutions, as described in Materials and Methods. The half maximal inhibitory concentrations (IC_{50}, 72 hour treatment) of fatostatin in LNCaP and C4-2B cells were 10.4 and 9.1 μmol/L, respectively (Fig. 1A). In addition, we determined the growth rate of each cell line by counting the total number of cells with or without fatostatin treatment. The growths of LNCaP and C4-2B cells were significantly inhibited by fatostatin in a dose- and time-dependent manner (Fig. 1B). Next, we examined the effect of fatostatin on the anchorage-independent colony formation ability in prostate cancer cells. After 3-week incubation, fatostatin notably inhibited the number and size of colony formation in LNCaP and C4-2B cells in a dose-dependent manner (Fig. 1C).

One of the hallmarks of progressive and metastatic cancer cells is their ability to invade surrounding tissues and migrate efficiently. The effect of fatostatin on the invasion and migration potentials of LNCaP and C4-2B cells was determined. After a 48-hour treatment, fatostatin significantly decreased the invasive (Fig. 1D) and migratory (Fig. 1E) capabilities of LNCaP and C4-2B cells compared with the untreated group. Take together; these data indicate that fatostatin inhibits proliferation, anchorage-independent colony formation, invasion, and migration in both androgen-responsive and androgen-independent prostate cancer cells.

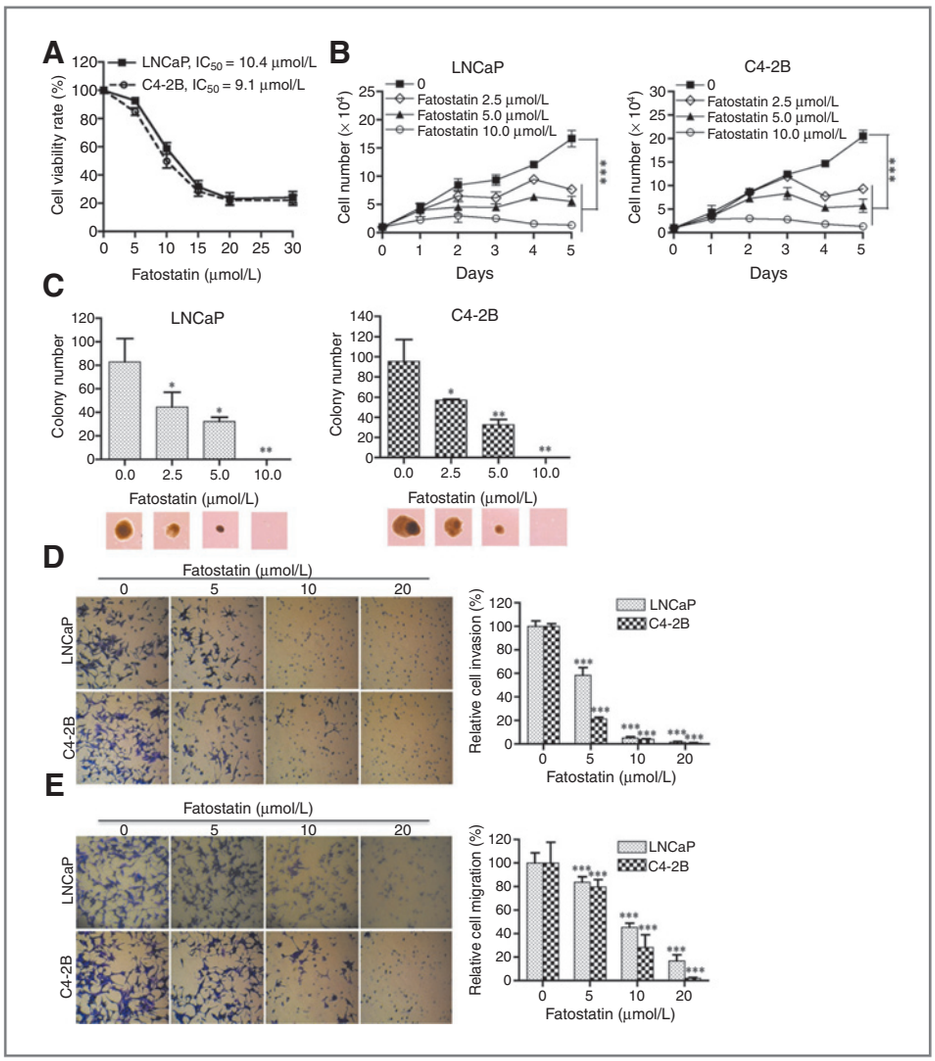

Figure 1. Fatostatin inhibits cell proliferation, colony formation, invasion, and migration of prostate cancer cells *in vitro*. A, fatostatin suppressed the proliferation of LNCaP and C4-2 B prostate cancer cells. The values are represented as percentage of viable cells where the vehicle-treated cells were regarded as 100%. The value of IC_{50} for a 72-hour treatment was calculated and is shown in the histogram. B, fatostatin inhibited the growth of LNCaP and C4-2B cells in a dose- (0–10 μmol/L) and time (0–5 days)-dependent manner. Cell growth was determined by counting cell numbers daily using a hemocytometer. C, fatostatin suppressed the anchorage-independent growth of LNCaP and C4-2B cells in a dose-dependent manner (0–10 μmol/L) for a 3-week treatment by the soft agar colony formation method. The number of colonies was counted and pictures of colony development were taken. Bars, mean ± SD of triplicate experiments. D and E, after a 48-hour treatment, fatostatin significantly decreased the invasive and migratory capabilities of LNCaP and C4-2B cells in a dose-dependent manner (0–20 μmol/L). The graphs show images of invading and migrating cells on the lower side of the inserts. *, $P < 0.05$; **, $P < 0.01$; ***, $P < 0.001$.

Fatostatin causes G_2–M cell-cycle arrest and induces caspase-mediated apoptosis in prostate cancer cells

The effects of fatostatin on cell-cycle distribution and apoptosis in prostate cancer cells were determined. LNCaP and C4-2B cells were exposed to various concentrations of fatostatin for 48 hours. Subsequently, the percentage of cell-cycle distribution was measured by flow cytometry–based PI staining. As shown in Fig. 2A, fatostatin induced a significant accumulation in the G_2–M phase in LNCaP and C4-2B cells. Next, the level of apoptosis induced by fatostatin was examined using simultaneous staining with FITC-coupled Annexin V and PI. The population of LNCaP and C4-2B cells in the early (bottom right) or late apoptotic (top right) stage was increased by fatostatin treatment (Fig. 2B). Only 1.84% or 0.57% of the late stage of apoptotic cells was detected in LNCaP or C4-2B without fatostatin treatment. However, the percentages of late apoptotic cells were significantly increased in both LNCaP (52.88%) and C4-2B (30.01%) cells after fatostatin (20 μmol/L) treatment.

To further define the mechanism underlying fatostatin-induced apoptotic cell death, we first examined a number of well-defined apoptotic markers involving caspase-3/7 enzymatic activity in prostate cancer cells by luminescence cleavage of specific substrates (Promega). A marked increase of caspase-3/7 enzymatic activities was found in LNCaP and C4-2B cells exposed to fatostatin with a dose-dependent manner (Fig. 2C). Next, we determined the expression patterns of caspases by Western blot analysis. Fatostatin decreased the expression of full-length caspases and increased the expression of cleaved caspase-9, caspase-3, and PARP, a downstream factor of caspases, in LNCaP and C4-2B cells (Fig. 2D). This indicates that fatostatin activates the apoptotic cascade pathway in prostate cancer cells. Collectively, these results suggest that fatostatin causes G_2–M cell-cycle arrest and induces caspase-dependent programmed cell death in LNCaP and C4-2B cells.

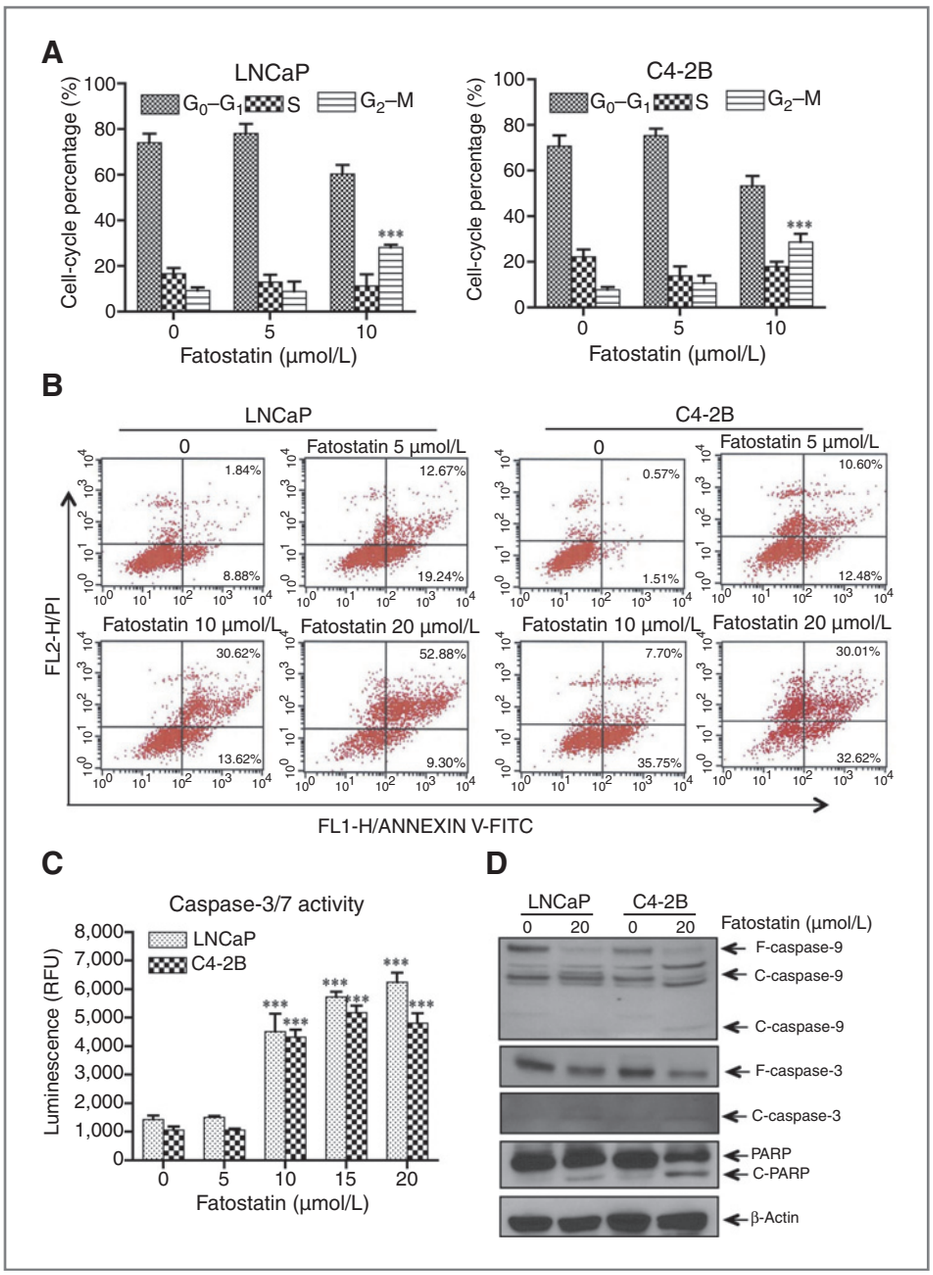

Figure 2. Fatostatin causes G_2–M cell-cycle arrest and induces apoptosis through caspase-mediated cleavages in prostate cancer cells. A, after 48-hour treatment, fatostatin induced G_2–M phase arrest in both LNCaP and C4-2B cells. The effect of fatostatin on cell-cycle distribution was determined by flow cytometry. Data represent the mean ± SD from triplicate experiments. B, after 48-hour treatment of fatostatin, LNCaP and C4-2B cells were stained with Annexin V-FITC and PI staining. C, fatostatin (0–20 μmol/L) induced caspase-3/7 activities in LNCaP and C4-2B cells. Fluorescent detection (RFU) of caspase-3/7 activities was measured using an enzymatic activity assay. Results represent the mean ± SD of triplicate experiments. ***, $P < 0.001$. D, fatostatin decreased full-length (F) caspase-9, caspase-3, and PARP, and increased cleaved (C) caspase-9, caspase-3, and PARP expression in LNCaP and C4-2B cells as assayed by Western blotting. β-Actin was used as a loading control.

Fatostatin inhibits SREBP processing and transcriptional activity, and key enzymes for lipogenesis and cholesterogenesis, to reduce fatty acid and cholesterol levels in prostate cancer cells

To reveal the molecular mechanism of fatostatin action in prostate cancer, we first investigated the nuclear translocation and transcriptional activity of SREBPs and their regulated anabolic pathways affected by fatostatin. As shown in Fig. 3A, expression of both nuclear SREBP-1 and SREBP-2 were decreased by fatostatin in a dose-dependent manner in LNCaP and C4-2B cells. In addition, immunofluorescence staining showed that fatostatin led to a reduction of SREBP-1 and SREBP-2 in the nuclear compartmentalization (Supplementary Fig. S2).

Next, we determined transcriptional expression of SREBP-controlled anabolic genes affected by fatostatin, including ACL, FASN, and SCD-1 for lipogenesis, HMGCS1, HMGCR, MVK, MVD, and LDLR for cholesterogenesis, two chaperones, INSIG1 and SCAP. As shown in Fig. 3B, fatostatin significantly downregulated mRNA expression of these genes in LNCaP and C4-2B cells. Fitting with the effects of fatostatin on SREBP target mRNA expression, FASN and HMGCR proteins were also suppressed by fatostatin in a dose-dependent pattern in prostate cancer cells (Fig. 3A).

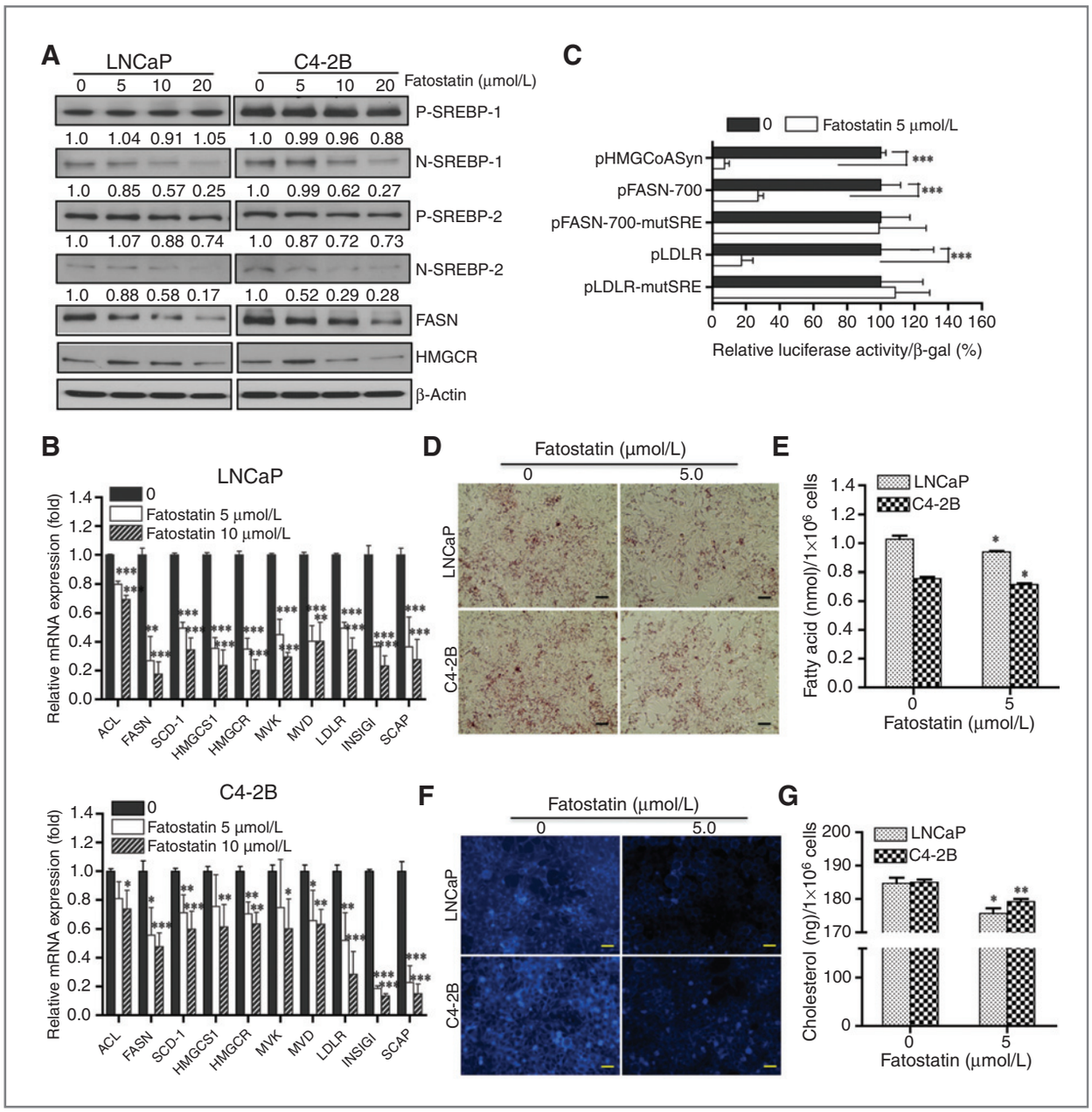

Figure 3. Fatostatin inhibits SREBP activation and regulated gene expression, and further reduces the levels of fatty acid and cholesterol in prostate cancer cells. A, precursor (P) and nuclear (N) forms of SREBP-1 and SREBP-2 were measured by Western blotting in LNCaP and C4-2B cells treated with vehicle or fatostatin for 24 hours. Nuclear SREBPs and expression of downstream proteins FASN and HMGCR were decreased by fatostatin in a dose-dependent pattern. β-Actin was used as a loading control. B, fatostatin decreased mRNA levels of ACL, FASN, SCD-1, HMGCS1, HMGCR, MVK, MVD, and LDLR and two chaperones, INSIG-1 and SCAP, in LNCaP and C4-2B cells examined by qRT-PCR. Data were normalized to β-actin and represent the mean ± SD of three independent duplicate experiments. *, $P < 0.05$; **, $P < 0.01$; ***, $P < 0.001$ significant differences from the absence of fatostatin. C, fatostatin decreased the activity of the HMGCoA Syn, FASN-700, and LDLR promoter-Luc reporter constructs, but did not affect the activity of the FASN-700-mutSRE and LDLR-mutSRE reporters. The relative luciferase activity was normalized by the β-galactosidase activity and assigned as 100% in the absence of fatostatin. ***, $P < 0.001$ significant differences from the absence of fatostatin. D and E, after treatment with vehicle or fatostatin for 48 hours, the levels of fatty acid in LNCaP and C4-2B cells were determined by Oil Red O staining and the Fatty Acid Quantification Kit. *, $P < 0.05$ significant differences from vehicle treatment; scale bar, 100 μm. F and G, after 48-hour incubation, fatostatin decreased the levels of cholesterols in LNCaP and C4-2B cells determined by the filipin staining and cholesterol quantitation kit. *, $P < 0.05$; **, $P < 0.01$ significant differences from vehicle group; scale bar, 100 μm.

To confirm that fatostatin acts on the SREBP pathways, the transcriptional ability of SREBP was determined by the promoter-luciferase (Luc) and mutant constructs assays for several SREBP-regulated genes. As shown in Fig. 3C, fatostatin significantly decreased the activities of the pHMGCoASyn-Luc, pFASN-700-Luc, and pLDLR-

Luc reporters, but not that of the mutant pFASN-700-mutSRE and pLDLR-mutSRE reporters. Moreover, the dominant negative SREBP forms (A-SREBP1 and A-SREBP2) were used to prove the specific effect of fatostatin on SREBP activation. Fatostatin significantly decreased the SRE-Luc activity in the presence of SREBP-1 or SREBP-2 expression vector but did not affect the SRE-Luc activity in the presence of dominant negative forms (Supplementary Fig. S3). The results indicated that fatostatin specifically blocked SREBP activation and processing.

Because fatostatin inhibited the key genes related to lipogenesis and cholesterogenesis through SREBPs, we subsequently performed staining and quantification assays to determine the changes of intracellular fatty acid and cholesterol levels caused by fatostatin treatment. The Oil Red O staining results showed that lipid droplet accumulation in fatostatin-treated LNCaP and C4-2B cells was decreased in comparison with vehicle-treated cells (Fig. 3D). In addition, fatostatin significantly decreased the levels of intracellular fatty acid compared with vehicle-treated cells (Fig. 3E). The filipin fluorescent staining demonstrated that cholesterol accumulation was decreased in fatostatin-treated cells compared with vehicle-treated prostate cancer cells (Fig. 3F). To further validate the results of the filipin fluorescent staining, we assayed the intracellular cholesterol levels in both cells. When LNCaP and C4-2B cells were exposed to fatostatin, total cholesterol amounts were significantly lower than vehicle-treated cells (Fig. 3G). These data suggest that inhibition of SREBPs by fatostatin caused a decrease in the levels of fatty acid and cholesterol in prostate cancer cells.

Fatostatin exhibits antitumor efficacy in a subcutaneous C4-2B xenograft mouse model

In view of the potent *in vitro* effect of fatostatin against prostate cancer cells (Figs. 1 and 2), we next examined the efficacy of fatostatin on human prostate cancer growth in immunodeficient mice. The volumes of subcutaneous C4-2 tumors treated with fatostatin were significantly smaller than those in the vehicle-treated control group over 42 days of observation (Fig. 4A). Moreover, at the end of the animal experiment, the average weight of the excised tumors collected from the fatostatin group was greatly decreased to 18% of the control group (Fig. 4B). Serum PSA levels of C4-2B tumor-bearing mice with fatostatin treatment were lower compared with control mice (Fig. 4C). In addition, the toxicity profile of fatostatin seemed quite favorable as body weight was not significantly affected by treatment with fatostatin compared with controls (Fig. 4D).

Next, we examined the proliferation (Ki67) and apoptosis (cleaved PARP) in C4-2B tumor tissues by IHC staining. Consistent with the potent antitumor effects, the results showed that the fatostatin-treated tumors exhibited a significant decrease in a proliferative index (Ki67 status) compared with the vehicle-treated group (Fig. 4E). A significant increase in cleaved PARP staining was observed in the fatostatin-treated tumors compared with the control tumors (Fig. 4E). The *in vivo* data suggest that the predominant effect of fatostatin on subcutaneous C4-2B tumors is inhibition of proliferation and induction of apoptosis.

Fatostatin exhibits significant *in vivo* antitumor activity by blocking SREBP-regulated metabolic pathways

Fatostatin has been demonstrated to inhibit fat biosynthesis and reduced body fat through SREBPs in obese mice (23). We subsequently determined expression of SREBP downstream target genes involved in lipogenesis and cholesterogenesis in the vehicle- and fatostatin-treated subcutaneous C4-2B tumors. The results of qRT-PCR showed that fatostatin significantly reduced mRNA levels of ACL, FASN, SCD-1, HMGCS1, HMGCR, MVK, MVD, INSIG1, and SCAP (Fig. 5A). In addition, expression of FASN and HMGCR proteins in tumors harvested from control and fatostatin-treated groups were examined by Western blot and IHC staining analysis. As shown in Fig. 5B and C, the expressions of HMGCR and FASN were lower in fatostatin-treated tumors than in vehicle-treated tumors. This suggests that fatostatin exerted its antitumor effects by decreasing the expression of SREBP target genes associated with biosynthesis of fatty acid and cholesterol in a xenograft mouse model, in accord with the observation that lipogenesis and cholesterogenesis have been shown to be linked with prostate cancer malignancy.

Fatostatin decreases expression of AR and its target gene PSA in prostate cancer *in vitro* and *in vivo*

AR activity is essential for prostate cancer development, growth, and castration-resistant progression. We previously showed that SREBP-1 transcriptionally induced AR expression and activity in prostate cancer cells (18). Here, we tested the idea that blocking SREBP-1 transcriptional activity by fatostatin inhibits the AR signaling in AR-positive LNCaP and C4-2B cells. As we expected, fatostatin affected the expression of AR and its downstream target gene PSA via dose-dependent inhibition in LNCaP and C4-2B cells (Fig. 6A). We also observed that fatostatin blocked AR nuclear translocation in both cell lines (Supplementary Fig. S4). Furthermore, the results of Western blot analysis at different time points showed that fatostatin first inhibited the nuclear translocation of SREBP-1 and SREBP-2 (at 6 hours) and subsequently decreased AR expression (at 12 hours) in LNCaP and C4-2B cells (Fig. 6B). It indicates that SREBPs are main targets of fatostatin, but not AR. Consistent with the *in vitro* results, fatostatin inhibited the expression of both AR and PSA compared with the vehicle group as determined by Western blot (Fig. 6C) and IHC staining (Fig. 6D) in a C4-2B tumor xenograft mouse model. In addition, the serum PSA levels of the fatostatin-treated mice were significantly reduced compared with the vehicle control group (Fig. 4C). These *in vitro* and *in vivo* results suggest that this specific SREBP

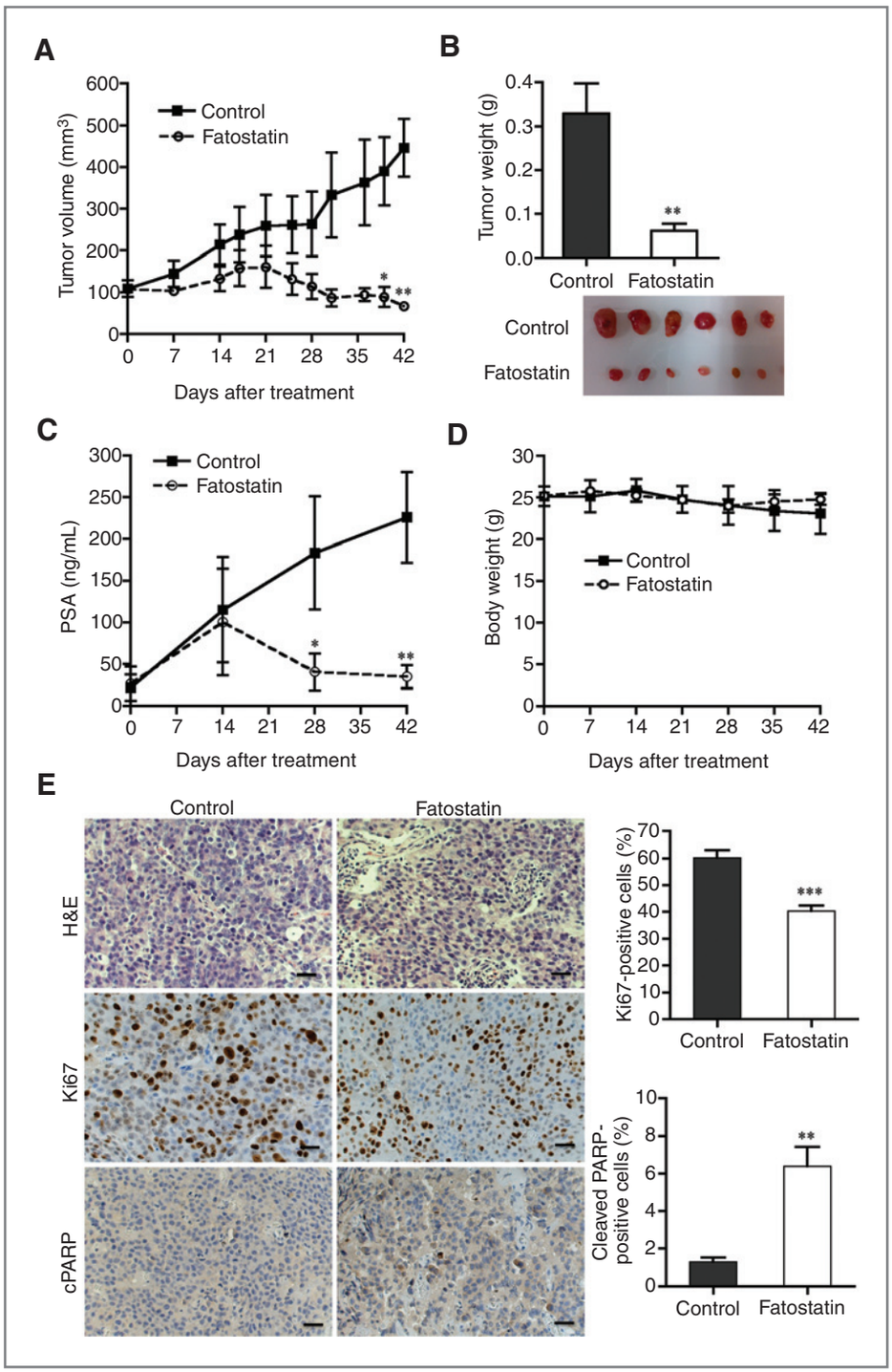

Figure 4. Fatostatin significantly suppresses subcutaneous C4-2B tumor growths in a xenograft tumor model. A and B, fatostatin significantly inhibited the growth and weight of subcutaneous C4-2B tumors compared with control vehicle-treated tumors during 6-week treatment ($n = 10$ for each group). Photograph of tumors in each group is shown. C, fatostatin reduced serum PSA levels compared with the control group. D, the body weights of mice displayed no differences between fatostatin and the control group. E, IHC staining results showed that decrease of Ki67 (cell proliferation) and increase of cleaved PARP (apoptosis) were observed in fatostatin-treated C4-2B tumors compared with control tumors; scale bar, 100 μm. Quantifications of Ki67 and cleaved PARP were analyzed by counting positive stained cells in an average of five random fields. *, $P < 0.05$; **, $P < 0.01$; ***, $P < 0.001$ significant differences from vehicle group. H&E, hematoxylin and eosin.

inhibitor inhibited AR expression and function in prostate cancer.

Discussion

Cancer cells reprogram the metabolic pathways to meet their abnormal demands for uncontrolled proliferation and survival. Accumulated research suggests that upregulation of *de novo* lipid synthesis is associated with prostate cancer malignancy (28, 29). The altered fatty acid and cholesterol biosynthesis in cancer cells regulated by oncogenic signaling pathways, tumor microenvironment, and metabolism-related transcription regulators are believed to be important for the initiation and progression of tumors (30, 31). Understanding the molecular mechanism for

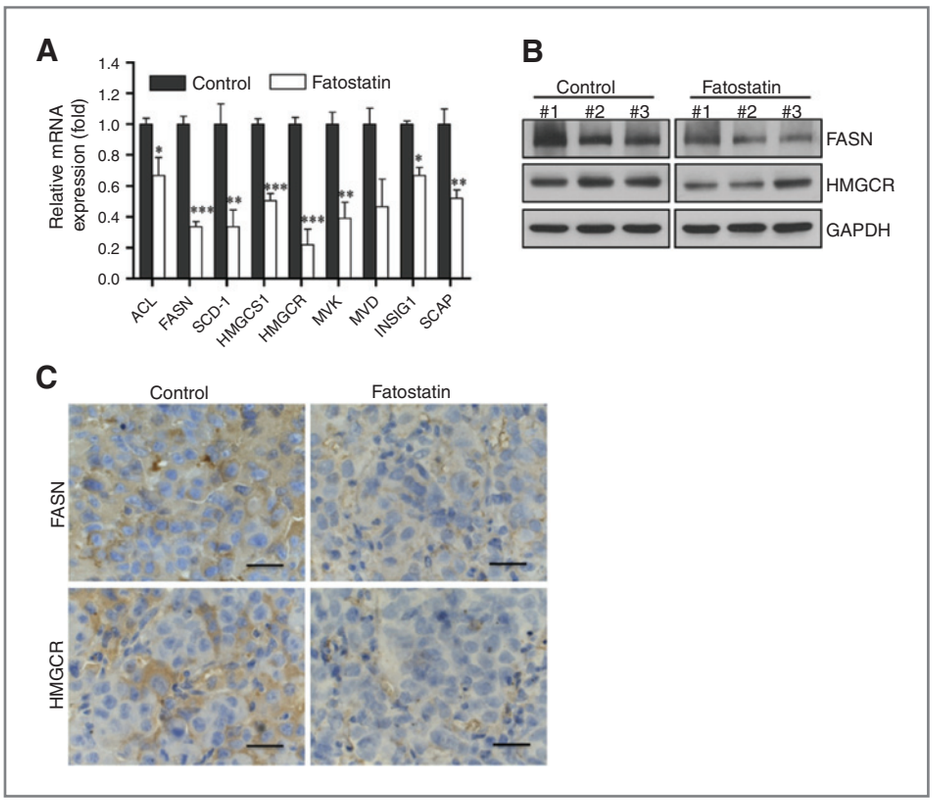

Figure 5. Fatostatin inhibits the mRNA and protein levels of SREBP downstream genes in C4-2B xenograft tumors. A, fatostatin inhibited mRNA expression of SREBP downstream target genes, including ACL, FASN, SCD-1, HMGCS1, HMGCR, MVK, and MVD and two chaperones, INSIG-1 and SCAP, compared with the control group. Total RNA was extracted from C4-2B xenograft tumors in nude mice treated with vehicle or fatostatin (4 tumors for each group). *, $P < 0.05$; **, $P < 0.01$; ***, $P < 0.001$ significant differences from vehicle-treated control tumors. B, Western blot analysis showed that fatostatin decreased expression of FASN and HMGCR in C4-2B xenograft tumors compared with the vehicle group. GAPDH was used as a loading control. C, the results of IHC staining showed that the expression of FASN and HMGCR was decreased in the fatostatin-treated C4-2B xenograft tumors compared with the vehicle group. Scale bar, 100 μm.

reprogramming lipogenesis and cholesterogenesis is the key to developing a successful therapy for eliminating prostate cancer.

SREBPs are transcription factors that predominantly activate expression of genes related to biosynthesis of long-chain fatty acid, triglyceride, and cholesterol and cholesterol uptake by binding to the SRE located in the 5′-flanking promoter region of these genes in the nucleus (32–34). Nuclear SREBP-1 proteolytic activation is under the control of hormones or signal transduction systems,

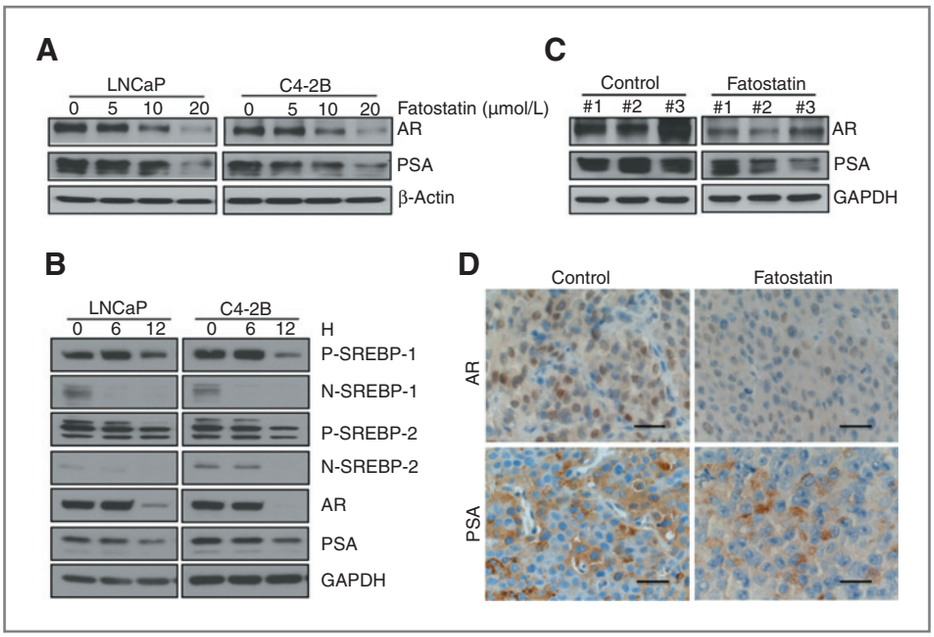

Figure 6. Fatostatin decreases expression of AR and its target gene PSA in prostate cancer cells and in a xenograft mouse model. A, after a 24-hour treatment, fatostatin inhibited the expression of AR and PSA in LNCaP and C4-2B cells in a dose-dependent manner. B, fatostatin (10 μmol/L) blocked activation of SREBP-1 and SREBP-2 (at 6 hours) and subsequently inhibited AR and PSA protein expression (at 12 hours) in LNCaP and C4-2B cells. P, precursor form; N, nuclear form. C, fatostatin also suppressed the expression of AR and PSA in C4-2B xenograft tumors compared with the vehicle group; GAPDH was used as a loading control. D, IHC staining showed that the expression of AR and PSA was reduced by fatostatin in C4-2B xenograft tumors. Scale bar, 100 μm.

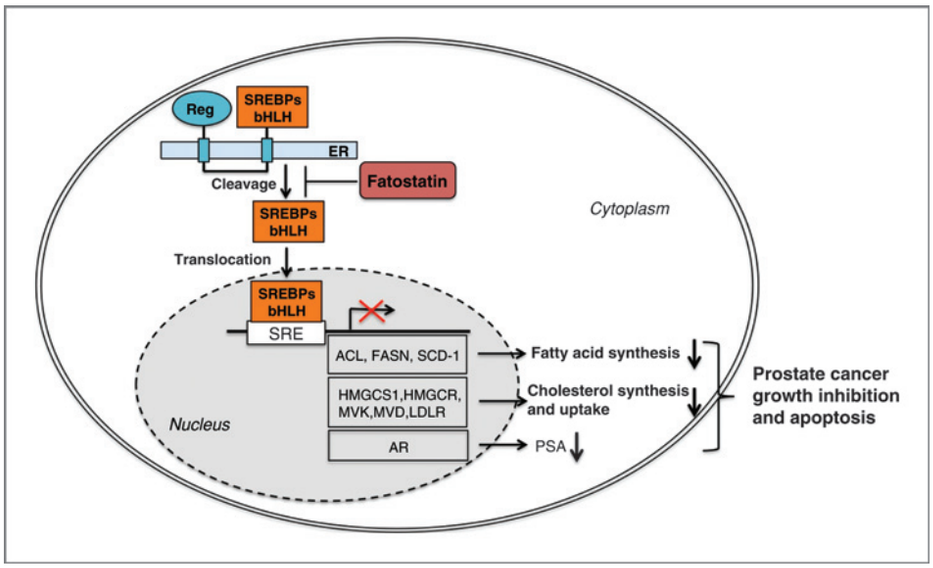

Figure 7. A proposed mechanism by which fatostatin inhibits prostate cancer growth and induces apoptosis by blocking activation of SREBPs, biosynthesis of fatty acid and cholesterol, and AR signaling. By inhibiting the nuclear translocation and transcriptional activity of SREBPs, fatostatin decreases the expression of SREBP downstream target genes, including FASN, SCD-1, HMGCS1, HMGCR, MVK, MVD, and LDLR, and further reduces the levels of intracellular fatty acid and cholesterol. In addition, fatostatin suppresses expression of AR and its target gene PSA. Through the concerted inhibition of lipogenesis, cholesterogenesis, and the AR signaling pathway, fatostatin inhibits cell proliferation and induces apoptosis in prostate cancer cells. Reg, regulatory domain.

and SREBP-2 nuclear translocation is regulated by the ER cholesterol content, reflecting its deep involvement in cholesterol homeostasis (35). SREBPs have been shown to promote prostate cancer growth, development, and progression. Importantly, clinical evidence revealed that overexpression of SREBP-1 and its nuclear form is associated with prostate cancer development and lethal castration resistance (17, 18). These experimental and clinical results offer a rationale for targeting SREBP transcriptional activity and regulated downstream metabolic pathways as a potential therapeutic approach for prostate cancer.

Transcription factors may be difficult to directly target by small molecules. However, the cytoplasmic maturation and nuclear translocation of SREBPs provides a feasible targeting approach. In the present study, a new SREBP blocker, fatostatin, was tested for anti–prostate cancer efficacy *in vitro* and *in vivo* by perturbing SREBP maturation and nuclear translocation. Fatostatin significantly inhibited cell proliferation and induced G_2–M cell-cycle arrest and caspase-dependent apoptosis in AR- and PSA-positive LNCaP and C4-2B prostate cancer cells. Fatostatin also suppressed subcutaneous C4-2B tumor growth and decreased serum PSA levels in a xenograft mouse model. Furthermore, through downregulation of SREBP-controlled metabolism-related enzymes, including FASN and HMGCR, fatostatin inhibited the levels of fatty acid and cholesterol in prostate cancer cells. Our data reveal an important and significant insight, that blocking the maturation and translocation of SREBPs provides a promising approach for perturbing the cancer metabolic program and attenuating prostate tumor growth.

Fatty acid is an essential constituent of all biologic membrane lipids and an important substrate for energy storage and metabolism. ACL, FASN, and SCD-1 are three primary enzymes at rate-limiting steps for biosynthesis of long-chain fatty acid. Markedly increased ACL expression and activity have been reported in cancer cells (36). FASN is highly expressed and associated with poor prognosis in human carcinomas including prostate cancer and has been considered as a metabolic oncogene (37–39). SCD-1 plays a critical role in the regulation of carcinogenesis, cancer cell proliferation, and programmed cell death (40). In this study, we demonstrated that fatostatin inhibited expression of ACL, FASN, and SCD-1 and the levels of intracellular fatty acid in prostate cancer cells and a xenograft tumor model. The inhibitory mechanism of fatostatin could be due to decreasing SREBP-1 transcriptional activity, as SREBP-1 has been demonstrated to transcriptionally mediate expression of these three lipogenic genes (12). The data suggest that fatostatin decreased the expression of cancer-associated lipogenic genes and further reduced intracellular fatty acid, to inhibit prostate cancer growth *in vitro* and *in vivo*.

Cholesterol is one of the major components of lipid rafts, specialized microdomains of the plasma membrane that serve as organizing centers for the assembly of signaling molecules (41). Therefore, rapidly proliferating cancer cells with highly activated signal transduction networks, such as prostate cancer cells, are likely to have an enhanced requirement for cholesterol (42). Besides, cholesterol is a metabolic precursor for biosynthesis of steroid hormones, including androgens. SREBP-2 is a master transcription regulator that upregulates several

key cholesterogenic genes, such as HMGCS1, HMGCR, and LDLR. HMGCR activity was increased in *ex vivo* LNCaP tumors during progression to a castration-resistant state in xenograft mouse models (43, 44). Expression of LDLR has been demonstrated to be elevated in prostate cancer cells compared with normal cells, which could be due to the lack of sterol feedback regulation controlled by SREBP-2 in prostate cancer cells (45). Blocking the intracellular cholesterol supply through inhibition of the LDLR pathway induced tumor cell death *in vivo* (46). Our results showed that inhibition of SREBP-2 activity by fatostatin suppressed the expression of these cholesterogenic genes and significantly reduced the levels of intracellular cholesterol in prostate cancer *in vitro* and *in vivo*, which is an essential component and precursor for the lipid raft–mediated survival signaling pathways and intracrine androgen biosynthesis. These results suggest that interrupting the SREBP-2–regulated cholesterogenic pathway may offer an attractive anti–prostate cancer approach.

Androgens exert their effects by interacting with AR to release HSPs and allowing nuclear localization and DNA interaction. AR, a critical transcription, growth, and survival factor, plays a key role in regulation of androgen-responsive organs during normal development and maintenance as well as prostate cancer growth and lethal hormone refractory/castration-resistant progression (47, 48). The AR signaling axis provides a promising targeted therapy for prostate cancer malignancy. Different strategies have been successfully attempted to target AR directly through gene transcription or translation or blocking the interaction between AR and its cofactors and their downstream functions in prostate cancer cells (26, 49). We previously reported that SREBP-1 mediated AR transcriptional expression and activity by a mechanism of binding the AR promoter region in prostate cancer cells (18). In addition, knocking down SREBP-1 led to decreases in AR mRNA and protein expression and inhibited prostate cancer cell viability (18, 27). Furthermore, unpublished results showed that silencing SREBP-2 by specific short hairpin RNA (shRNA) decreased expression of AR and its downstream target gene PSA in prostate cancer cells. These findings suggest that SREBPs could have an essential role as an important regulator for AR signaling. In this study, we demonstrated that interrupting SREBP activity by fatostatin suppressed the expression of AR and PSA in both androgen-responsive LNCaP and androgen-independent C4-2B cells. In a C4-2B xenograft mouse model, fatostatin also inhibited AR and PSA expression and decreased serum PSA levels. Taken together, the *in vitro* and *in vivo* results revealed an important mechanism by which fatostatin inhibited AR expression and activity via blockade and inhibition of the nuclear translocation and transcriptional activity of SREBP in prostate cancer cells. This could be exploited as a novel and improved therapeutic application by cotargeting the dysregulated metabolic pathways and the AR signaling axis using a SREBP inhibitor, such as fatostatin, to treat prostate cancer and hormone refractory/castration-resistant progression.

In summary, we uncovered the underlying molecular mechanisms by which fatostatin suppresses prostate cancer growth and tumorigenicity (Fig. 7). Fatostatin was shown to inhibit cell proliferation, anchorage-independent colony formation and progression, and induce the apoptotic pathway through interruption of SREBP nuclear translocation and transcriptional inhibition of SREBP-regulated metabolic gene expression and AR activity in both androgen-responsive and androgen-independent prostate cancer cells. These biologic effects of fatostatin provide a novel strategy for prostate cancer therapy. Future studies will determine the efficacy of fatostatin in advanced prostate cancer as well as various cancer types.

Disclosure of Potential Conflicts of Interest

No potential conflicts of interest were disclosed.

Authors' Contributions

Conception and design: X. Li, W.-C. Huang
Development of methodology: X. Li, Y.-T. Chen, P. Hu, W.-C. Huang
Acquisition of data (provided animals, acquired and managed patients, provided facilities, etc.): X. Li, Y.-T. Chen, P. Hu
Analysis and interpretation of data (e.g., statistical analysis, biostatistics, computational analysis): X. Li, Y.-T. Chen, P. Hu, W.-C. Huang
Writing, review, and/or revision of the manuscript: X. Li, W.-C. Huang
Administrative, technical, or material support (i.e., reporting or organizing data, constructing databases): X. Li, W.-C. Huang
Study supervision: W.-C. Huang

Acknowledgments

The authors thank Dr. Leland Chung and their colleagues at Cedars-Sinai Medical Center for helpful discussions and comments, and Gary Mawyer for editing the article. The authors also thank Dr. Timothy F. Osborne at Sanford-Burnham Medical Research Institute and Dr. Hitoshi Shimano at Tsukuba University for providing the promoter reporter constructs.

Grant Support

This work was supported by a grant from the Department of Defense (W81XWH-08-1-0321), the Cedars-Sinai Garber Awards for Cancer Science and NIH/National Center for Advancing Translational Sciences (NCATS, Grant # UL1TR000124; to W.-C. Huang).

The costs of publication of this article were defrayed in part by the payment of page charges. This article must therefore be hereby marked *advertisement* in accordance with 18 U.S.C. Section 1734 solely to indicate this fact.

Received September 23, 2013; revised December 18, 2013; accepted January 20, 2014; published OnlineFirst February 3, 2014.

References

1. Baade PD, Youlden DR, Krnjacki LJ. International epidemiology of prostate cancer: geographical distribution and secular trends. Mol Nutr Food Res 2009;53:171–84.
2. Siegel R, Naishadham D, Jemal A. Cancer statistics, 2012. CA Cancer J Clin 2012;62:10–29.
3. Mistry T, Digby JE, Desai KM, Randeva HS. Obesity and prostate cancer: a role for adipokines. Eur Urol 2007;52:46–53.
4. Giovannucci E, Rimm EB, Colditz GA, Stampfer MJ, Ascherio A, Chute CC, et al. A prospective study of dietary fat and risk of prostate cancer. J Natl Cancer Inst 1993;85:1571–9.

5. Whittemore AS, Kolonel LN, Wu AH, John EM, Gallagher RP, Howe GR, et al. Prostate cancer in relation to diet, physical activity, and body size in blacks, whites, and Asians in the United States and Canada. J Natl Cancer Inst 1995;87:652–61.
6. Swinnen JV, Heemers H, van de Sande T, de Schrijver E, Brusselmans K, Heyns W, et al. Androgens, lipogenesis and prostate cancer. J Steroid Biochem Mol Biol 2004;92:273–9.
7. Swinnen JV, Heemers H, Heyns W, Verhoeven G. Androgen regulation of lipogenesis. Adv Exp Med Biol 2002;506:379–87.
8. Zhang F, Du G. Dysregulated lipid metabolism in cancer. World J Biol Chem 2012;3:167–74.
9. Mittal A, Sathian B, Chandrasekharan N, Lekhi A, Yadav SK. Role of hypercholesterolemia in prostate cancer–case control study from Manipal Teaching Hospital Pokhara, Nepal. Asian Pac J Cancer Prev 2011;12:1905–7.
10. Shafique K, McLoone P, Qureshi K, Leung H, Hart C, Morrison DS. Cholesterol and the risk of grade-specific prostate cancer incidence: evidence from two large prospective cohort studies with up to 37 years' follow up. BMC Cancer 2012;12:25.
11. Hager MH, Solomon KR, Freeman MR. The role of cholesterol in prostate cancer. Curr Opin Clin Nutr Metab Care 2006;9:379–85.
12. Shimano H. Sterol regulatory element-binding proteins (SREBPs): transcriptional regulators of lipid synthetic genes. Prog Lipid Res 2001;40:439–52.
13. Brown MS, Goldstein JL. The SREBP pathway: regulation of cholesterol metabolism by proteolysis of a membrane-bound transcription factor. Cell 1997;89:331–40.
14. Sakai J, Duncan EA, Rawson RB, Hua X, Brown MS, Goldstein JL. Sterol-regulated release of SREBP-2 from cell membranes requires two sequential cleavages, one within a transmembrane segment. Cell 1996;85:1037–46.
15. Osborne TF. Sterol regulatory element-binding proteins (SREBPs): key regulators of nutritional homeostasis and insulin action. J Biol Chem 2000;275:32379–82.
16. Shimano H, Shimomura I, Hammer RE, Herz J, Goldstein JL, Brown MS, et al. Elevated levels of SREBP-2 and cholesterol synthesis in livers of mice homozygous for a targeted disruption of the SREBP-1 gene. J Clin Invest 1997;100:2115–24.
17. Ettinger SL, Sobel R, Whitmore TG, Akbari M, Bradley DR, Gleave ME, et al. Dysregulation of sterol response element-binding proteins and downstream effectors in prostate cancer during progression to androgen independence. Cancer Res 2004;64:2212–21.
18. Huang WC, Li X, Liu J, Lin J, Chung LW. Activation of androgen receptor, lipogenesis, and oxidative stress converged by SREBP-1 is responsible for regulating growth and progression of prostate cancer cells. Mol Cancer Res 2012;10:133–42.
19. Krycer JR, Kristiana I, Brown AJ. Cholesterol homeostasis in two commonly used human prostate cancer cell-lines, LNCaP and PC-3. PLoS ONE 2009;4:e8496.
20. Krycer JR, Phan L, Brown AJ. A key regulator of cholesterol homoeostasis, SREBP-2, can be targeted in prostate cancer cells with natural products. Biochem J 2012;446:191–201.
21. Li X, Chen YT, Josson S, Mukhopadhyay NK, Kim J, Freeman MR, et al. MicroRNA-185 and 342 inhibit tumorigenicity and induce apoptosis through blockade of the SREBP metabolic pathway in prostate cancer cells. PLoS ONE 2013;8:e70987.
22. Choi Y, Kawazoe Y, Murakami K, Misawa H, Uesugi M. Identification of bioactive molecules by adipogenesis profiling of organic compounds. J Biol Chem 2003;278:7320–4.
23. Kamisuki S, Mao Q, Abu-Elheiga L, Gu Z, Kugimiya A, Kwon Y, et al. A small molecule that blocks fat synthesis by inhibiting the activation of SREBP. Chem Biol 2009;16:882–92.
24. Williams KJ, Argus JP, Zhu Y, Wilks MQ, Marbois BN, York AG, et al. An essential requirement for the SCAP/SREBP signaling axis to protect cancer cells from lipotoxicity. Cancer Res 2013;73:2850–62.
25. Thalmann GN, Sikes RA, Wu TT, Degeorges A, Chang SM, Ozen M, et al. LNCaP progression model of human prostate cancer: androgen-independence and osseous metastasis. Prostate 2000;44:91–103.
26. Huang WC, Havel JJ, Zhau HE, Qian WP, Lue HW, Chu CY, et al. Beta2-microglobulin signaling blockade inhibited androgen receptor axis and caused apoptosis in human prostate cancer cells. Clin Cancer Res 2008;14:5341–7.
27. Huang WC, Zhau HE, Chung LW. Androgen receptor survival signaling is blocked by anti-beta2-microglobulin monoclonal antibody via a MAPK/lipogenic pathway in human prostate cancer cells. J Biol Chem 2010;285:7947–56.
28. Menendez JA, Lupu R. Fatty acid synthase and the lipogenic phenotype in cancer pathogenesis. Nat Rev Cancer 2007;7:763–77.
29. Swinnen JV, Brusselmans K, Verhoeven G. Increased lipogenesis in cancer cells: new players, novel targets. Curr Opin Clin Nutr Metab Care 2006;9:358–65.
30. Tennant DA, Duran RV, Gottlieb E. Targeting metabolic transformation for cancer therapy. Nat Rev Cancer 2010;10:267–77.
31. Cairns RA, Harris IS, Mak TW. Regulation of cancer cell metabolism. Nat Rev Cancer 2011;11:85–95.
32. Horton JD, Goldstein JL, Brown MS. SREBPs: activators of the complete program of cholesterol and fatty acid synthesis in the liver. J Clin Invest 2002;109:1125–31.
33. Horton JD, Shah NA, Warrington JA, Anderson NN, Park SW, Brown MS, et al. Combined analysis of oligonucleotide microarray data from transgenic and knockout mice identifies direct SREBP target genes. Proc Natl Acad Sci U S A 2003;100:12027–32.
34. Sakai J, Nohturfft A, Goldstein JL, Brown MS. Cleavage of sterol regulatory element-binding proteins (SREBPs) at site-1 requires interaction with SREBP cleavage-activating protein. Evidence from in vivo competition studies. J Biol Chem 1998;273:5785–93.
35. Sato R. Sterol metabolism and SREBP activation. Arch Biochem Biophys 2010;501:177–81.
36. Hatzivassiliou G, Zhao F, Bauer DE, Andreadis C, Shaw AN, Dhanak D, et al. ATP citrate lyase inhibition can suppress tumor cell growth. Cancer Cell 2005;8:311–21.
37. Kuhajda FP. Fatty acid synthase and cancer: new application of an old pathway. Cancer Res 2006;66:5977–80.
38. Bandyopadhyay S, Pai SK, Watabe M, Gross SC, Hirota S, Hosobe S, et al. FAS expression inversely correlates with PTEN level in prostate cancer and a PI 3-kinase inhibitor synergizes with FAS siRNA to induce apoptosis. Oncogene 2005;24:5389–95.
39. Shah US, Dhir R, Gollin SM, Chandran UR, Lewis D, Acquafondata M, et al. Fatty acid synthase gene overexpression and copy number gain in prostate adenocarcinoma. Hum Pathol 2006;37:401–9.
40. Igal RA. Stearoyl-CoA desaturase-1: a novel key player in the mechanisms of cell proliferation, programmed cell death and transformation to cancer. Carcinogenesis 2010;31:1509–15.
41. Simons K, Toomre D. Lipid rafts and signal transduction. Nat Rev Mol Cell Biol 2000;1:31–9.
42. Zhuang L, Lin J, Lu ML, Solomon KR, Freeman MR. Cholesterol-rich lipid rafts mediate akt-regulated survival in prostate cancer cells. Cancer Res 2002;62:2227–31.
43. Leon CG, Locke JA, Adomat HH, Etinger SL, Twiddy AL, Neumann RD, et al. Alterations in cholesterol regulation contribute to the production of intratumoral androgens during progression to castration-resistant prostate cancer in a mouse xenograft model. Prostate 2010;70:390–400.
44. Locke JA, Wasan KM, Nelson CC, Guns ES, Leon CG. Androgen-mediated cholesterol metabolism in LNCaP and PC-3 cell lines is regulated through two different isoforms of acyl-coenzyme A: Cholesterol Acyltransferase (ACAT). Prostate 2008;68:20–33.
45. Chen Y, Hughes-Fulford M. Human prostate cancer cells lack feedback regulation of low-density lipoprotein receptor and its regulator, SREBP2. Int J Cancer 2001;91:41–5.
46. Guo D, Reinitz F, Youssef M, Hong C, Nathanson D, Akhavan D, et al. An LXR agonist promotes glioblastoma cell death through inhibition of an EGFR/AKT/SREBP-1/LDLR-dependent pathway. Cancer Discov 2011;1:442–56.
47. Heinlein CA, Chang C. Androgen receptor in prostate cancer. Endocr Rev 2004;25:276–308.
48. Dehm SM, Tindall DJ. Regulation of androgen receptor signaling in prostate cancer. Expert Rev Anticancer Ther 2005;5:63–74.
49. Chang CY, McDonnell DP. Androgen receptor-cofactor interactions as targets for new drug discovery. Trends Pharmacol Sci 2005;26:225–8.